Organic Light-Emitting Diode Based Fluorescence Sensing System for DNA Detection

Cheng Lian, Kou Yoshida, Claude Nogues,* and Ifor D. W. Samuel*

Conventional fluorescence sensing equipment for disease detection is expensive and bulky, restricting access of patients to accurate diagnosis. Organic light-emitting diodes (OLEDs) have the potential to enable compact fluorescence sensing compatible with point-of-care (POC) testing. However, the limited brightness and broad emission spectra of OLEDs can be a challenge for achieving good sensitivity. Here, co-host microcavity OLEDs with narrowed spectra, high conductivity, and high brightness are developed for fluorescence sensing. The OLEDs are driven in pulsed mode for achieving higher brightness and stable light output. To sense the presence of single-stranded DNA (ssDNA), two complementary ssDNA labelled with Cyanine dyes – Cy3 (ssDNA-Cy3) or Cy5 (ssDNA-Cy5) are used to form a Förster resonance energy transfer (FRET) pair when the DNA hybridized. The dye-labelled DNA is then excited by the OLED at the Cy3 excitation wavelength, and the fluorescence is detected at the emission wavelength of Cy5. As a result, the device shows a very high sensitivity that can detect as low as 1×10^{-9} M of ssDNA-Cy5 in fetal bovine serum (FBS). This work shows a simple approach to highly sensitive fluorescence sensing with OLED light sources that is promising for use in POC diagnostics.

1. Introduction

Over the past decades, there has been a significant increase in human lifespan due to the progress in public health.[1] Disease detection with advanced diagnostic technologies such as

C. Lian, K. Yoshida, I. D. W. Samuel
Organic Semiconductor Centre
SUPA
School of Physics and Astronomy
University of St. Andrews
St. Andrews KY16 9SS, UK
E-mail: idws@st-andrews.ac.uk
C. Nogues
Laboratoire de Biologie et Pharmacologie appliquée
CNRS (UMR 8113)
IDA (FR 3242)
ENS Paris-Saclay
Université Paris-Saclay
Gif-sur-Yvette 91190, France
E-mail: claude.nogues@kimialys.com

enzyme-linked immunoabsorbent assay (ELISA) and quantitative polymerase chain reaction (qPCR) is often expensive, cumbersome, and time-consuming. This means it is not available in primary care. In addition, the imbalance of healthcare resources between developed and developing countries[2], limits the access of people living in developing countries to such advanced diagnostics.[3] Therefore, it is desirable to employ technologies that are cheap to produce and deploy, portable with rapid feedback of results while maintaining the device sensitivity and robustness uncompromised.

A point-of-care (POC) diagnostic test is a medical laboratory diagnostic test intended to be carried out in the direct vicinity of the patients, with the result obtained in a short time (30 to 60 min). In addition, these tests should be designed to be carried out by personnel who are not trained in a medical laboratory, such as medical assistants or patients themselves. One of the most common examples of POC devices is the lateral flow device (LFD) for pregnancy test, which only needs a few drops of a urine sample to indicate pregnancy in a very short time. In the pregnancy test LFD, gold nanoparticles are used as the indicator to show the results with visual inspection of line color.[4] It gives a qualitative result with relatively low-cost and simple readout method. To further improve the system for more sensitive and quantitative measurement, optical systems with fluorescent detection have been developed.[5] In fluorescence sensing, a light source excites the fluorescence of a dye-labelled analytes. Fluorescence sensing has advantages of low-background, fast-response, and is widely used in diagnostics. Therefore, the basic components to perform fluorescence sensing at least involves a light source and a detector. However, most fluorescence sensing systems use bulky and expensive equipment such as lasers, filtered lamp, photomultiplier, microscope, and spectrometers to enhance the sensitivity of system, which are difficult to be integrated into a compact device for POC purpose. Light-emitting diodes (LEDs) are being explored as potential compact light sources for POC fluorescence.[6–8]

Organic light-emitting diodes (OLEDs) are made from thin layers of organic semiconductors. They are promising candidates for POC fluorescence sensing because they are compact, lightweight, thin and can easily be integrated with other sensing components.[9,10] OLEDs have several advantages compared to their inorganic counterparts. They are simple to make by thermal evaporation at moderate temperature, and

room temperature deposition and patterning of organic semiconductors is possible by processes such as ink-jet printing or blade-coating, while LED fabrication typically involves the much more complicated process of epitaxial growth at much higher temperature. The simpler fabrication methods such as ink-jet printing can also lead to low-cost devices and potentially (if desired) disposable devices.[11,12] Furthermore, OLEDs can be patterned on a single substrate with multiple customized pixel geometries because they are intrinsically area light sources while LEDs are only point light sources.[13] As OLEDs do not involve epitaxial growth, different color pixels can be patterned side by side on the same substrate, enabling different dyes to be excited for biosensing. Hence, multiplexed tests for different diseases could be achievable using high-density OLED pixels with customized shapes and different colors. An integrated device for testing simultaneously different biomarkers and diagnosing different diseases at the same time would be very attractive. It would be simple, effective and make it much easier for patients and doctors to access the testing. Consequently, the easier fabrication process and flexible design strategy can potentially make OLEDs more suitable light sources compared to inorganic LEDs for some applications.

Recently, many new perspectives have been brought by OLED-based biomedical applications such as photodynamic therapy,[14,15] photobiomodulation,[16,17] imaging,[18] muscle contraction sensing,[19] optogenetics,[20,21] and health-monitoring.[22,23] In terms of fluorescence sensing, a few examples of miniaturized system using OLEDs have been demonstrated as POC or lab-on-a-chip devices.[11,13,24–31] Since the commonly used dyes in fluorescence sensing have small Stokes shift,[32] a narrow spectrum of excitation light source is required to distinguish the excitation and detection light. However, OLEDs generally show broader emission spectra and lower brightness than inorganic LEDs, which are issues that need to be overcome for successful fluorescence sensing.[33,34]

In this paper, we developed a very sensitive OLED-based fluorescence sensing device for the detection of dye-labelled DNA. The device includes an OLED as excitation light source, an excitation filter, an emission filter, and a photodiode as readout. To obtain high fluorescence signal minimizing background noise, we designed the OLED structure to be high-brightness and have narrow emission spectra by using a p-i-n top-emitting structure with co-host emission layer. To achieve even higher brightness, the OLED was pulsed. As a result, our OLED-based fluorescence sensing system has a high sensitivity, and can detect 1×10^{-9} M of DNA in fetal bovine serum (FBS).

2. Cy3 and Cy5 as Fluorescent Dyes for DNA Hybridization Sensing

To demonstrate the potential of the OLED-based fluorescence sensing device, we used two complementary single-stranded DNA segments (ssDNA) each labelled with fluorophores that undergo Förster resonance energy transfer (FRET) when hybridized to form double-stranded DNA (dsDNA). The ideal fluorescent dyes would have high extinction coefficient, high quantum yield and good photostability. The cyanine dye, Cy3, was chosen as the dye for the fluorescence sensing system due to its adequate fluorescence quantum yield and good photostability.[35] However, Cy3 has a small Stokes shift: the photoluminescence excitation (PLE) peak is at 548 nm while the emission peak is at 565 nm (**Figure 1**a). To overcome the issue of small Stokes shift, we take the advantage of FRET between Cy3 (the donor) and Cy5 (the acceptor) to effectively increase the Stokes shift. By using FRET, the peak excitation wavelength is still 548 nm while the peak emission wavelength of Cy5 is 667 nm (Figure 1a). Consequently, the OLED emission can be well-resolved from the emission of the acceptor (Cy5) when exciting at the donor (Cy3) excitation wavelengths, which reduces the background noise from OLED emission. In addition, efficient FRET can be expected due to the significant spectral overlap between the photoluminescence (PL) spectrum of Cy3 and the photoluminescence excitation (PLE) spectrum of Cy5.

In this study, two complementary single-stranded DNA (ssDNA) are labelled with Cy3 (ssDNA-Cy3) and Cy5 (ssDNA-Cy5). The ssDNA-Cy3 (donor) is here considered as the capture molecule and is kept at a constant concentration. The ssDNA-Cy5 (acceptor) is therefore the target molecule that can be mixed with the capture ssDNA at different concentrations.
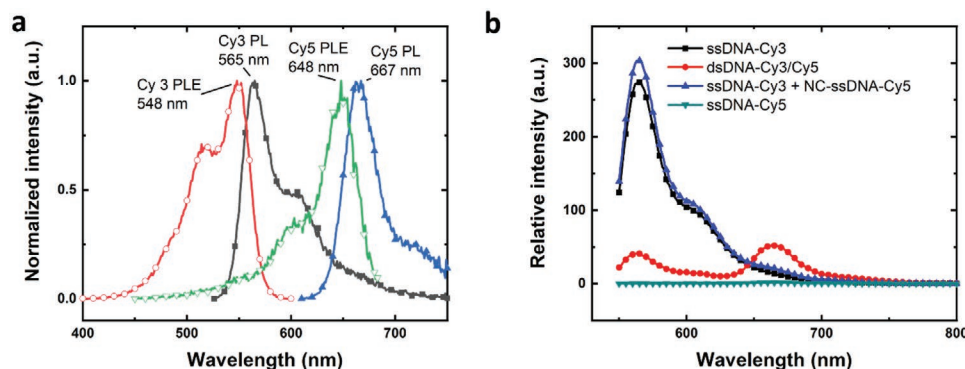

Figure 1. Cy3 and Cy5 as labeling dyes for fluorescence sensing. a) Normalized PL and PLE spectra of dsDNA-Cy3 and dsDNA-Cy5 at 1×10^{-6} M in PBS. The PL excitation wavelengths were 516 and 600 nm for dsDNA-Cy3 and dsDNA-Cy5, respectively, and the PLE detection wavelengths were 610 and 668 nm for dsDNA-Cy3 and dsDNA-Cy5, respectively. b) PL spectra of 50×10^{-9} M of dye-labelled DNA in PBS excited at 516 nm. The samples used in the experiments are ssDNA-Cy3, ssDNA-Cy5, dsDNA-Cy3/Cy5 (hybridized double-stranded DNA with Cy3 attached on one complementary strand and Cy5 attached on another). The non-complementary strands are a mixture of 50×10^{-9} M ssDNA-Cy3 and 50×10^{-9} M NC-ssDNA-Cy5.

Since the two ssDNA are complementary, they hybridized to form the dsDNA and the distance between Cy3 and Cy5 is reduced. This turns on FRET from Cy3 to Cy5 and gives an increase in Cy5 fluorescence signal. By monitoring the Cy5 fluorescence intensity, we can determine the presence of ssDNA-Cy5 in solution and have access to a quantitative estimation since the emission intensity of Cy5 is proportional to the amount of complementary ssDNA in solution. Figure 1b shows the emission spectra of ssDNA-Cy3 alone and the emission spectra of the dsDNA-Cy3/Cy5 (hybridized from the equal concentration of ssDNA-Cy3 and ssDNA-Cy5) diluted in phosphate-buffered saline (PBS). The excitation wavelength was set to 516 nm, which can only excite Cy3 efficiently, and the emission spectra were measured between 550 and 800 nm to detect the emission of both ssDNA-Cy3 and ssDNA-Cy5. The ssDNA-Cy3 shows a maximum emission intensity at 563 nm with a shoulder at 600 nm. After hybridization with the ssDNA-Cy5, the emission from the Cy3 decreases significantly and emission from the Cy5 is clearly detected. We can also observe that there is almost no increase in Cy5 emission for ssDNA-Cy3 mixed with non-complementary ssDNA-Cy5 (NC-ssDNA-Cy5), which suggests no FRET happens when DNA are not hybridized. The Figure 1b shows that direct excitation of ssDNA-Cy5 at 516 nm is negligible as it shows no Cy5 peak in the PL spectrum. These results show that hybridization of ssDNA-Cy3 and ssDNA-Cy5 leads to FRET that makes Cy5 emission detectable when exciting at 516 nm.

3. Development of OLEDs for Fluorescence Sensing

To achieve sensitive fluorescence sensing, high brightness and suitable emission wavelength are very important parameters for the excitation light source. To have the efficient excitation of Cy3, we used a green phosphorescent emitter bis[2-(2-pyridinyl-N)phenyl-C](acetylacetonato)iridium(III) [Ir(ppy)$_2$(acac)] for OLED fabrication. OLEDs with p-doped and n-doped transport layers (p-i-n OLEDs) using the same emitter molecules have been previously reported with high efficiency.[36] In the present work, we applied a similar structure but with further development to achieve higher brightness as shown in **Figure 2**a. We first started with a bottom-emitting architecture, D1. In this structure, indium tin oxide (ITO) was used as the transparent anode and aluminum (Al) is the opaque cathode. We used 2,2′,7,7′-tetra(N,N-di-p-tolyl)amino-9,9-spirobifluorene (Spiro-TTB) doped by 2,2-(per-fluoronaphthalene-2,6-diylidene)dimalononitrile (F6-TCNNQ) as hole transport layer (HTL), 1,1-bis[(di-4-tolylamino) phenyl]cyclohexane (TAPC) as electron blocking layer (EBL), 4,7-diphenyl-1,10-phenanthroline (BPhen) as hole blocking layer and BPhen doped by cesium (Cs) as electron transport layer (ETL). The emission layer (EML) consisted of 8 wt% of Ir(ppy)$_2$(acac) doped into tris(4-carbazoyl-9-ylphenyl)amine (TCTA) which we noted it as EML A. The structure of D1 is ITO/ Spiro-TTB: F6-TCNNQ (4 wt%)/ TAPC/ EML A/ BPhen/ BPhen: Cs/ Al as shown in Figure 2a. As a result, D1 has an emission peak at 525 nm which is suitable for exciting Cy3 (Figure 2b). However, a long emission tail is present in the

D1 emission spectrum, which is not desirable as the emission tail longer than 550 nm will be cut off by our excitation filter (Figure 2b) and will not contribute to the excitation of Cy3. Thus, light sources with narrowed emission spectra are preferable for fluorescence sensing as they can target the absorption peaks of dyes more efficiently. Meanwhile, the remaining emission tail from the OLEDs can be rejected by an excitation filter, which lowers the background noise for fluorescence sensing.

To narrow the emission spectra of the OLEDs, we designed top-emitting microcavity device, D2: Al/ Spiro-TTB: F6-TCNNQ (4 wt%)/ TAPC/ EML A/ BPhen/ BPhen: Cs/ Ag/ $N,N′$-di(1-naphthyl)-$N,N′$-diphenyl-(1,1′-biphenyl)-4,4′-diamine (NPB), which has 80 nm Al opaque bottom electrodes and 20 nm semi-transparent silver top electrodes acting as reflective mirrors (Figure 2a). D2 showed a narrower emission spectrum narrowing at the optimal wavelength compared to D1 as we carefully tuned the microcavity by changing HTL thickness (see Figure 2b and Figure S1: Supporting Information for more details). In combination with a p-i-n structure, a narrowed emission spectrum with suitable peak wavelength was achieved without changing the conductivity of the devices.[15]

To enhance the brightness of our OLEDs, we introduced a co-host EML structure. The structure of device D3 was Al/ Spiro-TTB: F6-TCNNQ (4 wt%)/ TAPC/ EML B/ BPhen/ BPhen: Cs/ Ag/ NPB. EML B represents the emission layer with 8 wt% of Ir(ppy)$_2$(acac) doped in TCTA and BPhen as co-host (Figure 2a). As shown in Figure 2b, D2 and D3 have similar narrow emission spectrum with an emission peak at 523 nm. The current density–voltage–luminance (J–V–L) characteristics of the OLEDs are shown in Figure 2c. D3 shows much higher current density at the same driving voltage compared to D1 and D2, which results in a higher luminance. Moreover, D3 also exhibits a higher current efficiency under the same luminance than D1 and D2 (Figure 2d). Here, we attribute the better performance of D3 to the co-host structure. It is known that a co-host structure can reduce the charge injection barrier and improve the charge balance, which enables low driving voltage and high efficiency.[37] In addition, the improvement in driving voltage and current efficiency can reduce Joule heating of the OLEDs, and so enable them to operate at higher brightness.[38] Hence, we chose device D3 for our sensing study.

Although the device with co-host structure, D3, shows better performance than the others, it can degrade especially at high driving voltage because of heat generation[38,39] and the short operational lifetime due to the co-host structure.[40] Thus, the maximum brightness is limited when the OLEDs are driven continuously. However, fluorescence sensing does not require continuous illumination, so we explored pulsed excitation. We operated our OLEDs with square voltage pulses with a width of 300 µs at 10 Hz so that the OLEDs can survive even at very high current density (Figure 2e). By using pulsed operation, we achieved over 700 000 cd m^{-2} at 16.2 V and current density of 7660 mA cm^{-2}. The stability of device performance under pulse operation was tested at applied voltage of 16.2 V by checking luminance from the OLED after the stated number of pulse (Figure 2f). After 6000 pulses, we observed a degradation of 3.2% from the initial luminance, which is stable enough to be used in fluorescence sensing.
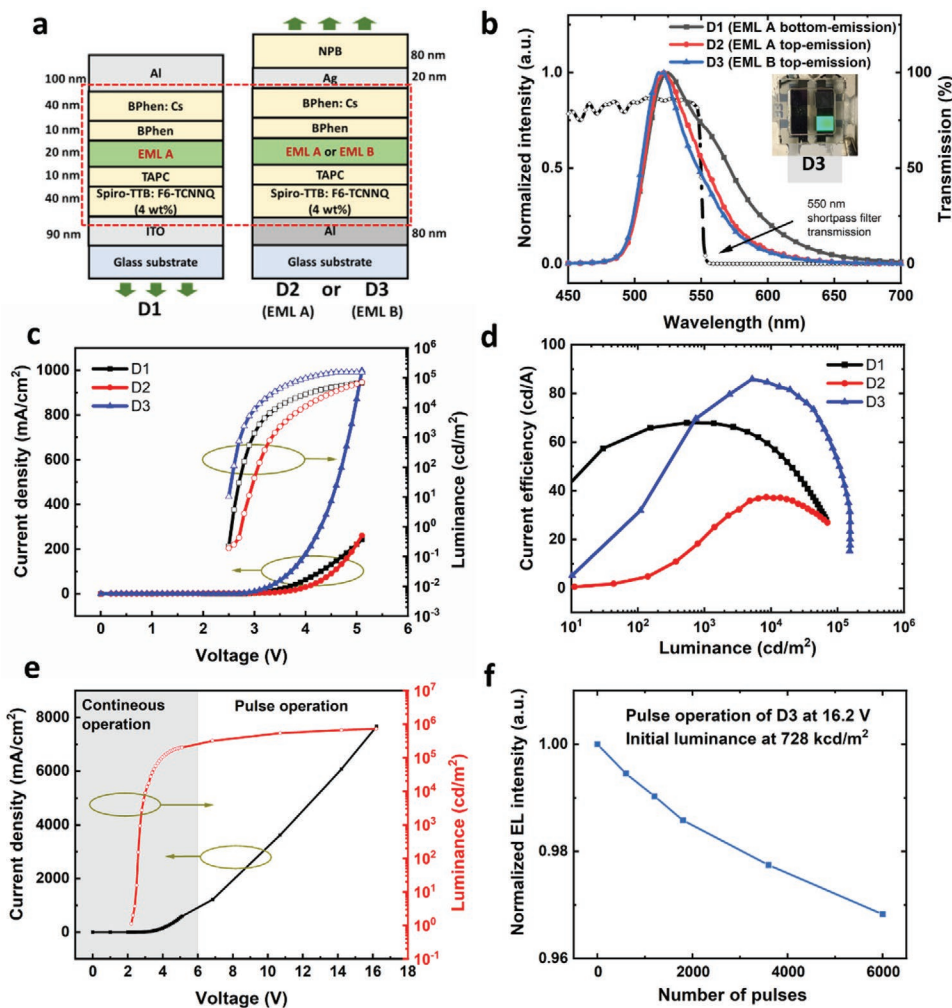
Figure 2. Development of OLEDs for fluorescence sensing. a) OLED structures of bottom-emission and top-emission device with different emission layers. EML A is a single host emission layer with 8 wt% Ir(ppy)$_2$(acac) in TCTA host; EML B is a co-host emission layer with TCTA: BPhen: Ir(ppy)$_2$(acac) (0.46: 0.46: 0.08 in wt%). Device 1 (D1): bottom-emission structure with EML A. Device 2 (D2): top-emission structure with EML A. Device 3 (D3): top-emission structure with EML B. b) Electroluminescence (EL) spectra of D1, D2, D3 and transmission spectrum of the short-pass filter. Inset photo showing green emission from D3. c) J–V–L characteristics of D1, D2, and D3. d) Current efficiency versus luminance of D1, D2, and D3. e) J–V–L characteristics of OLEDs operated under continuous mode and pulse mode. f) Luminance change versus pulse number of the D3-OLED driven in pulse mode.

4. Fluorescence Sensing with OLEDs

4.1. Fluorescence Sensing Setup

To realize POC testing, we developed a compact fluorescence sensing setup as shown in **Figure 3**a. The dye-labelled DNA was diluted in a buffer solution and put into plastic cuvettes. The main parts of the setup consisted of the D3-OLED as the excitation light source, a 550 nm short-pass interference filter to cut off the OLED emission tail, a 3D printed sample holder to fix the cuvette, a 650 nm long-pass interference filter to avoid the excitation light reaching the detector, and a silicon photodiode with a variable gain transimpedance amplifier. The photo in Figure S2 (Supporting Information) shows the main part of our sensing system, which is only a bit bigger than the normal USB stick.

The D3-OLED was pulsed to excite the sample, and fluorescence was detected by the amplified photodiode whose voltage was read out by an oscilloscope. Then, the measured data were processed by a computer to calculate the results such as the detection limit. To evaluate the sensitivity of the setup, we used signal-to-noise-ratio (SNR) to compare the level of fluorescence signal and the level of background noise. It is defined as

$$SNR = \frac{S-B}{SD_{S-B}},$$ where S is the raw fluorescence signal, B is the

background signal, and SD_{S-B} is the standard deviation of fluorescence signal with background subtracted ($S - B$). We note that, instead of using standard deviation of just background signal, we calculated the noise from SD_{S-B}. This is because the fluctuations of fluorescence signal can also contribute to the noise (Table S1, Supporting Information). Finally, the gain of the photodiode was optimized to maximize signal to noise ratio
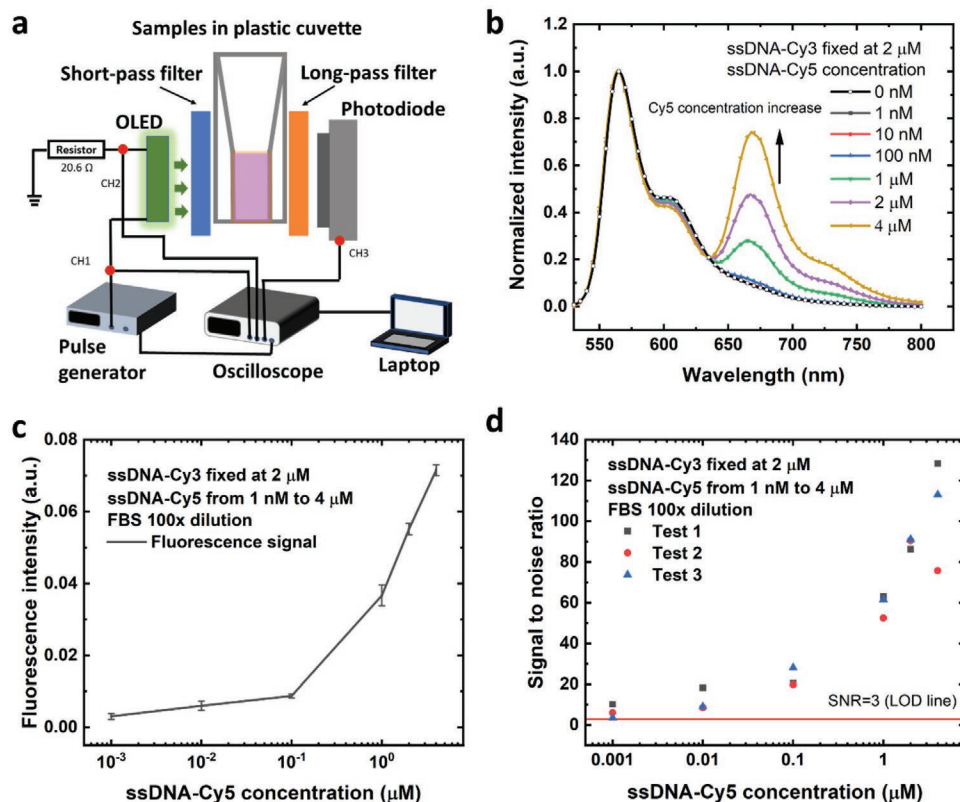
Figure 3. a) Schematic diagram of fluorescence sensing system with the OLED as excitation light source. b) Normalized PL spectra measured with the fluorimeter excited at 516 nm for ssDNA-Cy3 concentration fixed at 2×10^{-6} M and a range of ssDNA-Cy5 concentrations in 100xFBS. c) Fluorescence signal under OLED excitation when ssDNA-Cy3 fixed at 2×10^{-6} M and ssDNA-Cy5 at different concentrations in 100xFBS. The mean and standard deviation of the fluorescence signal is shown. d) *SNR* calculated from the fluorescence sensing results when ssDNA-Cy3 fixed at 2×10^{-6} M and ssDNA-Cy5 at different concentrations in 100xFBS (three tests with the same sample for each concentration).

as shown in Table S1 (Supporting Information). A gain setting of 70 dB was found to be best for all the remaining fluorescence sensing measurements.

4.2. Fluorescence Linearity Test of dsDNA-Cy3/Cy5 with OLED Excitation

To evaluate the sensitivity of our sensing system, we performed the experiments in 100 times diluted fetal bovine serum (100xFBS) in deionized water, which is a complex medium that generates higher background noise than PBS. We prepared different solution of dsDNA-Cy3/Cy5 in 100xFBS at following concentrations: 100×10^{-12} M, 1×10^{-9} M, 10×10^{-9} M, 100×10^{-9} M, 1×10^{-6} M, and 2×10^{-6} M. To estimate the reproducibility of the measurements, three samples were prepared for each concentration. The samples were first measured in a commercial fluorimeter to confirm that FRET was taking place. FRET was successfully observed in samples with concentrations from 1×10^{-9} M to 2×10^{-6} M (Figure S3a, Supporting Information). However, it is not clear whether there is FRET in the 100×10^{-12} M sample as it is reaching the detection limit of the fluorimeter. Then, dsDNA-Cy3/Cy5 samples were measured in our sensing system under OLED excitation. The limit of detection (LOD) is the lowest concentration of a substance that can be detected.

We defined this as the concentration where $SNR = 3$. The fluorescence signals tested with OLED excitation showed a linear relationship at low dsDNA-Cy3/Cy5 concentrations but a sublinear behaviour when it reaches 2×10^{-6} M (Figure S3b, Supporting Information). We attribute the sublinear behavior at the high concentrations to the higher optical density as the dye fluorescence travels longer distance inside the cuvette. Thus, the fluorescence signal is not proportional to the dsDNA-Cy3/Cy5 concentration. The *SNR* of three repetitions with different concentrations were then calculated (Figure S3c, Supporting Information) and the LOD of dsDNA-Cy3/Cy5 was estimated to be $1-10 \times 10^{-9}$ M (Table S2, Supporting Information). The detailed *SNR* of each repetition at different concentrations is summarized in Table S3 (Supporting Information).

4.3. Fluorescence Sensing of ssDNA-Cy5 with OLED Excitation

The sensing performance of the device was tested by mixing a fixed concentration of ssDNA-Cy3 with different concentrations of ssDNA-Cy5 in 100xFBS. The concentration of ssDNA-Cy3 was fixed at 2×10^{-6} M, and then 1×10^{-9} M, 10×10^{-9} M, 100×10^{-9} M, 1×10^{-6} M, 2×10^{-6} M, and 4×10^{-6} M of ssDNA-Cy5 were added into the ssDNA-Cy3 solution, respectively, for hybridization. Additionally, a sample with 2×10^{-6} M of ssDNA-Cy3 only was

**ADVANCED
SCIENCE NEWS**
www.advancedsciencenews.com

**ADVANCED
MATERIALS
TECHNOLOGIES**
www.advmattechnol.de

prepared as a reference. The spectra of these hybridized dye-labelled DNA samples were first measured in the fluorimeter and FRET was observed (Figure 3b). As we normalized the spectra at Cy3 emission peak, we observed the increase in Cy5 emission as the ssDNA-Cy5 concentration increased, which indicates more FRET pairs were formed at higher ssNDA-Cy5 concentration. Next, we measured dye-labelled DNA under OLED excitation with our fluorescence sensing device and three repetitive tests were done for each sample. As shown in Figure 3c, the fluorescence signal increased as the concentration of ssDNA-Cy5 increased, which is consistent with the results measured with the fluorimeter. Furthermore, the measured fluorescence signals at each concentration have a relatively small variation, which makes quantitative tests possible at the stated concentration range. The *SNR* was calculated as shown in Figure 3d. As a result, all the three repetitions showed that 1×10^{-9} M of ssDNA-Cy5 can be detected when mixed with 2×10^{-6} M of ssDNA-Cy3 using our system. To investigate how ssDNA-Cy3 concentration affects the results, we fixed the ssDNA-Cy3 at 100 and 500×10^{-9} M, respectively, to hybridize with varied concentrations of ssDNA-Cy5. Figure S4 (Supporting Information) shows the PL spectra, fluorescence intensity and *SNR* when the concentration of ssDNA-Cy3 was fixed at 100 or 500×10^{-9} M and the details of *SNR* are shown in Tables S4,S5, and S6 (Supporting Information). As summarized in **Table 1**, the lowest concentration of ssDNA-Cy5 can be detected when 2×10^{-6} M ssDNA-Cy3 was used. This is probably due to more ssDNA-Cy3 being available to hybridize with ssDNA-Cy5. Similar measurements were also done under the same concentrations with PBS as buffer solution (Figure S5, Supporting Information). As PBS is a simple isotonic solution that has a lower background noise compared to FBS, we achieved even higher *SNR* using PBS when fixing ssDNA-Cy3 at 2×10^{-6} M (Table S7, Supporting Information) – for example we were able to detect 1×10^{-9} M ssDNA-Cy5 with an *SNR* (averaged over 3 tests) of 14.

Finally, we compared the LOD of our system with the reported results on miniaturized fluorescence sensing systems based on inorganic LEDs or OLEDs as excitation light sources. Reported LODs of LED-based systems were 1.96 and 3×10^{-9} M, detected with photodiodes.[6,7] In the OLED-based systems, LOD of 3×10^{-6} M was achieved with photomultiplier detector;[25] 10×10^{-9} M was reached with lock-in amplifier and organic photodiodes;[11] 3×10^{-9} M was achieved with quantum dots as fluorophores and a digital camera as detector.[29] A direct comparison of these reports with each other and with our work is difficult because of the different optical configurations used and analytes detected,

but the 1×10^{-9} M LOD we achieve is encouraging. We can envisage a range of further improvements in the sensitivity and practicality of our system as follows. In our system, the fluorescence quantum yield of Cy3 and Cy5 (0.24 and 0.2) are much lower than that of the fluorophores used in other works such as rhodamine 6G (0.91) and fluorescein (0.89).[41,42] Thus, the fluorescence signal can be further improved by using dyes with higher quantum yield. Furthermore, by using dyes with larger Stokes shift such as R-phycoerythrin,[43] or OLED emitter material with narrow emission spectra,[44] noise from OLED can be further reduced without compromising OLED brightness. Additionally, the size of our device is only a bit larger than a USB stick. At present the pulse generator and oscilloscope are conventional lab instruments but they could be replaced by compact battery-powered electronics. According to related works, we can even make our system more compact by making OLEDs smaller, detecting different biomarkers on a single chip,[7] and using organic photodiodes as detectors.[11] We believe our results show that OLEDs are promising for POC testing, and further developments on device compactness, sensitivity and stability can be made as they are developed for clinical use.

5. Conclusion

In conclusion, we developed a compact dye-labelled DNA sensing system using OLEDs as excitation sources. The device includes an OLED light source, an excitation filter, an emission filter, and a photodiode detector. The OLEDs were optimized with a top-emitting p-i-n structure for narrower spectra and high conductivity. They were further enhanced by using co-host emission layer to obtain higher brightness and current efficiency. To deliver higher brightness and avoid device breakdown due to Joule heating, we operated the OLEDs with pulsed voltage. To address the small Stokes shift of dyes, we used Cy3/Cy5 FRET pair in our DNA sensing system so that OLED emission can be well-separated from the fluorescence signal. Furthermore, fluorescence sensing of ssDNA-Cy5 was demonstrated with the OLEDs as excitation light source using fixed concentration of ssDNA-Cy3 to hybridize with different concentrations of ssDNA-Cy5 in 100xFBS. As a result, we achieved a high sensitivity using the OLED excitation, which can detect 1×10^{-9} M of ssDNA-Cy5 when mixing with 2×10^{-6} M of ssDNA-Cy3. It is also found that the limit of detection can be further improved by increasing the fixed concentration of ssDNA-Cy3. This proof of principle of sensitive DNA detection using OLEDs can be developed to provide sensitive fluorescent detection of a wide range of diseases. For example, target DNA and RNA can be detected by intercalating specific fluorophores or fluorophores interacting specifically with double strand DNA. Proteins could be detected by the fluorescence of readout antibodies. Our fluorescence sensing device is simple and compact, and shows that OLEDs are promising for point-of-care diagnosis of disease.

6. Experimental Section

Dye-Labelled DNA Hybridization and Sensing Sample Preparation: Dye-labelled DNA strands were purchased from Eurgentec with an initial

Table 1. Calculated LOD of the OLED fluorescence sensing system when ssDNA-Cy3 at a fixed concentration and ssDNA-Cy5 at different concentrations (T1, T2, and T3 represent the results of three repetitive tests).

ssDNA-Cy3 concentration	LOD		
[μM]	T1	T2	T3
	[nM]	[nM]	[nM]
0.1	6.5	7.3	5.4
0.5	6.1	17	1.2
2	<1	<1	<1

**ADVANCED
SCIENCE NEWS**

www.advancedsciencenews.com

**ADVANCED
MATERIALS
TECHNOLOGIES**

www.advmattechnol.de

concentration of 100×10^{-6} M in deionized water. They were further diluted with 100xFBS or PBS to obtain the desirable concentrations for experiment. The dsDNA-Cy3/Cy5 were prepared from ssDNA-Cy3 mixed with ssDNA-Cy5 in FBS or PBS, and the mixed solution was water bathed at 92–95°C for 2–5 min. Then, the solution was cooled down overnight before any measurement to get an effective DNA hybridization. After that, 70 μL of the sample solution was loaded into a plastic cuvette for measurement.

PL and PLE Spectroscopies of Dye-Labelled DNA: PL and PLE of dye-labelled DNA were measured in a cuvette by fluorimeters (FLS980, Edinburgh Instruments or Cary Eclipse, Varian). In Figure 1a, the PL excitation wavelengths for dsDNA-Cy3 and dsDNA-Cy5 were 516 and 600 nm, respectively, the PLE detection wavelengths for dsDNA-Cy3 and dsDNA-Cy5 were 610 and 668 nm, respectively. For the rest of the PL spectra in this work, the PL excitation wavelength was 516 nm.

OLED Fabrication: OLEDs were deposited by thermal evaporation (EvoVac, Angstrom Engineering Inc.) under a base pressure of 3×10^{-7} mbar. The Al anode was deposited at 3 Å s^{-1}; HTL was deposited at 0.6 Å s^{-1}; emission layer was deposited at 0.3 Å s^{-1}; HBL and EBL were at 0.3 Å s^{-1}; ETL and Ag cathode were at 1 Å s^{-1}; Al anode was at 3 Å s^{-1}; NPB capping layer was at 2 Å s^{-1}. After deposition, OLEDs were encapsulated under nitrogen atmosphere with glass lids and epoxy glue.

OLED Characterization: The electroluminescence spectra of the OLEDs were obtained using a spectrograph (MS125, Oriel) connected to a charge coupled device (CCD) camera (DV420-BU, Andor). The electrical performance of OLEDs at continuous driving mode were measured with a source meter (Keithley 2400, Keithley), and the optical performance was measured with a multimeter (Keithley 2000, Keithley) and a calibrated Si photodiode. OLED performance under pulse operation was measured with a pulse generator (HP 8114A, Hewlett Packard), an oscilloscope (MSO 3014, Tektronix), and a Si photodiode (PDA100A-EC, Thorlabs). The current during pulsed operation was estimated from the voltage drop across a 20.5 Ω resistor connected in series with the OLED. The voltage applied to the OLED was calculated by using the total voltage produced from the pulse generator (CH1) and subtracting the voltage drop across the resistor (CH2) from the total voltage. The OLED current was calculated by dividing the voltage drop across the resistor by 20.5 Ω.

Fluorescence Sensing Measurement: The D3-OLED was driven in pulsed mode with a width of 300 μs at 10 Hz. The pulse voltage applied on the OLED was calculated to be 16.2 V by subtracting the voltage drop across the resistor from the total voltage generated from the pulse generator. A short-pass filter (FES0550, Thorlabs) was used to cut-off the long-wavelength emission tail from OLED and a long-pass filter (FELH0650, Thorlabs) was used to stop the excitation light coming into the detector. The fluorescence from dye-labelled DNA was read out with a Si photodiode (PDA100A-EC, Thorlabs) connected to the oscilloscope and further calculation of fluorescence signal and signal to noise ratio were processed by a computer.

Statistical Analysis: The emission and absorption spectra were normalized between 0 and 1. The results for fluorescence sensing are expressed as mean value ± standard deviation. The sample sizes of the tests are shown in the caption of each Figure.

Supporting Information

Supporting Information is available from the Wiley Online Library or from the author.

Conflict of Interest

C.N. is co-founder and shareholder of Kimialys, a company developing surface chemistry applied to biosensors.

[1] E. M. Crimmins, *Gerontologist* **2015**, *55*, 901.
[2] P. Yager, T. Edwards, E. Fu, K. Helton, K. Nelson, M. R. Tam, B. H. Weigl, *Nature* **2006**, *442*, 412.
[3] V. Gubala, L. F. Harris, A. J. Ricco, M. X. Tan, D. E. Williams, *Anal. Chem.* **2012**, *84*, 487.
[4] K. M. Koczula, A. Gallotta, *Essays Biochem.* **2016**, *60*, 111.
[5] F. B. Myers, L. P. Lee, *Lab Chip* **2008**, *8*, 2015.
[6] L. Novak, P. Neuzil, J. Pipper, Y. Zhang, S. Lee, *Lab Chip* **2007**, *7*, 27.
[7] G. Ryu, J. Huang, O. Hofmann, C. A. Walshe, J. Y. Y. Sze, G. D. McClean, A. Mosley, S. J. Rattle, J. C. DeMello, A. J. DeMello, D. D. C. Bradley, *Lab Chip* **2011**, *11*, 1664.
[8] M. Yamazaki, S. Krishnadasan, A. J. Demello, J. C. Demello, *Lab Chip* **2012**, *12*, 4313.
[9] M. S. White, M. Kaltenbrunner, E. D. Głowacki, K. Gutnichenko, G. Kettlgruber, I. Graz, S. Aazou, C. Ulbricht, D. A. M. Egbe, M. C. Miron, Z. Major, M. C. Scharber, T. Sekitani, T. Someya, S. Bauer, N. S. Sariciftci, *Nat. Photonics* **2013**, *7*, 811.
[10] C. Keum, C. Murawski, E. Archer, S. Kwon, A. Mischok, M. C. Gather, *Nat. Commun.* **2020**, *11*, 6250.
[11] A. Pais, A. Banerjee, D. Klotzkin, I. Papautsky, *Lab Chip* **2008**, *8*, 794.
[12] I. Titov, M. Kopke, N. C. Schneidewind, J. Buhl, Y. Murat, M. Gerken, *IEEE Sens. J.* **2020**, *20*, 7540.
[13] A. Marcello, D. Sblattero, C. Cioarec, P. Maiuri, P. Melpignano, *Biosens. Bioelectron.* **2013**, *46*, 44.
[14] S. K. Attili, A. Lesar, A. McNeill, M. Camacho-Lopez, H. Moseley, S. Ibbotson, I. D. W. Samuel, J. Ferguson, *Br. J. Dermatol.* **2009**, *161*, 170.
[15] C. Lian, M. Piksa, K. Yoshida, S. Persheyev, K. J. Pawlik, K. Matczyszyn, I. D. W. Samuel, *npj Flexible Electron.* **2019**, *3*, 18.
[16] X. Wu, S. Alberico, E. Saidu, S. Rahman Khan, S. Zheng, R. Romero, H. Sik Chae, S. Li, A. Mochizuki, J. Anders, *Wound Repair Regen.* **2015**, *23*, 104.
[17] Y. Jeon, H.-R. Choi, J. H. Kwon, S. Choi, K. M. Nam, K. Park, K. C. Choi, *Light: Sci. Appl.* **2019**, *8*, 114.
[18] C. Murawski, A. Mischok, J. Booth, J. D. Kumar, E. Archer, L. Tropf, C. Keum, Y. Deng, K. Yoshida, I. D. W. Samuel, M. Schubert, S. R. Pulver, M. C. Gather, *Adv. Mater.* **2019**, *31*, 1903599.
[19] A. K. Bansal, S. Hou, O. Kulyk, E. M. Bowman, I. D. W. Samuel, *Adv. Mater.* **2015**, *27*, 7638.
[20] A. Steude, E. C. Witts, G. B. Miles, M. C. Gather, *Sci. Adv.* **2016**, *2*, 1600061.
[21] C. Murawski, S. R. Pulver, M. C. Gather, *Nat. Commun.* **2020**, *11*, 6248.
[22] C. M. Lochner, Y. Khan, A. Pierre, A. C. Arias, *Nat. Commun.* **2014**, *5*, 5745.
[23] T. Yokota, P. Zalar, M. Kaltenbrunner, H. Jinno, N. Matsuhisa, H. Kitanosako, Y. Tachibana, W. Yukita, M. Koizumi, T. Someya, *Sci. Adv.* **2016**, *2*, 1501856.

[24] B. Choudhury, R. Shinar, J. Shinar, *J. Appl. Phys.* **2004**, *96*, 2949.

[25] B. Yao, G. Luo, L. Wang, Y. Gao, G. Lei, K. Ren, L. Chen, Y. Wang, Y. Hu, Y. Qiu, *Lab Chip* **2005**, *5*, 1041.

[26] O. Hofmann, P. Miller, P. Sullivan, T. S. Jones, J. C. Demello, D. D. C. Bradley, A. J. Demello, *Sens. Actuators, B* **2005**, *106*, 878.

[27] B. Lamprecht, T. Abel, E. Kraker, A. Haase, C. Konrad, M. Tscherner, S. Köstler, H. Ditlbacher, T. Mayr, *Phys. Status Solidi RRL* **2010**, *4*, 157.

[28] H. Nakajima, Y. Okuma, K. Morioka, M. Miyake, A. Hemmi, T. Tobita, M. Yahiro, D. Yokoyama, C. Adachi, N. Soh, K. Nakano, S. Xue, H. Zeng, K. Uchiyama, T. Imato, *J. Sep. Sci.* **2011**, *34*, 2906.

[29] V. Venkatraman, A. J. Steckl, *Biosens. Bioelectron.* **2015**, *74*, 150.

[30] B. A. Katchman, J. T. Smith, U. Obahiagbon, S. Kesiraju, Y.-K. Lee, B. O'Brien, K. Kaftanoglu, J. Blain Christen, K. S. Anderson, *Sci. Rep.* **2016**, *6*, 29057.

[31] J. T. Smith, B. A. Katchman, D. E. Kullman, U. Obahiagbon, Y. Lee, B. P. O'Brien, G. B. Raupp, K. S. Anderson, J. B. Christen, *J. Disp. Technol.* **2016**, *12*, 273.

[32] Z. Gao, Y. Hao, M. Zheng, Y. Chen, *RSC Adv.* **2017**, *7*, 7604.

[33] M. Jahnel, B. Beyer, M. Thomschke, K. Fehse, F. Krujatz, K. Leo, *Electronics* **2015**, *4*, 982.

[34] S.-M. Yang, P.-H. Wang, C.-H. Chao, C.-W. Chu, Y.-T. Yeh, Y.-S. Chen, F.-P. Chang, Y.-H. Fang, C.-C. Lin, C.-I. Wu, *Opt. Express* **2019**, *27*, A1308.

[35] R. Roy, S. Hohng, T. Ha, *Nat. Methods* **2008**, *5*, 507.

[36] C. Murawski, C. Fuchs, S. Hofmann, K. Leo, M. C. Gather, *Appl. Phys. Lett.* **2014**, *105*, 113303.

[37] J. H. Lee, H. Shin, J. M. Kim, K. H. Kim, J. J. Kim, *ACS Appl. Mater. Interfaces* **2017**, *9*, 3277.

[38] P. Tyagi, R. Srivastava, L. I. Giri, S. Tuli, C. Lee, *Synth. Met.* **2016**, *216*, 40.

[39] K. J. Bergemann, R. Krasny, S. R. Forrest, *Org. Electron.* **2012**, *13*, 1565.

[40] S. K. Jeon, H. L. Lee, K. S. Yook, J. Y. Lee, *Adv. Mater.* **2019**, *31*, 1803524.

[41] J. Malicka, I. Gryczynski, J. Fang, J. R. Lakowicz, *Anal. Biochem.* **2003**, *317*, 136.

[42] C. Würth, M. Grabolle, J. Pauli, M. Spieles, U. Resch-Genger, *Nat. Protoc.* **2013**, *8*, 1535.

[43] M. Munier, S. Jubeau, A. Wijaya, M. Morançais, J. Dumay, L. Marchal, P. Jaouen, J. Fleurence, *Food Chem.* **2014**, *150*, 400.

[44] T. Hatakeyama, K. Shiren, K. Nakajima, S. Nomura, S. Nakatsuka, K. Kinoshita, J. Ni, Y. Ono, T. Ikuta, *Adv. Mater.* **2016**, *28*, 2777.

2100806 (8 of 8)